



ChemComm

Electronic Supplementary Information

Ranking of Keggin- and Dawson-type polyoxometalates in the Hofmeister series according to their ability to adsorb on polar neutral surfaces

Thomas Buchecker,^a Philipp Schmid,^a Séverine Renaudineau,^c Olivier Diat,^b Anna Proust,^c Arno Pfitzner^{a*} and Pierre Bauduin^{b*}

- a. Institute of Inorganic Chemistry, University of Regensburg, 93040 Regensburg, Germany.
E-mail: arno.pfitzner@chemie.uni-regensburg.de
- b. Institut de chimie séparative de Marcoule (ICSM), UMR 5257 (CEA, CNRS, UM, ENSCM), BP 17171, 30207 Bagnols-sur-Cèze, France. E-mail Pierre.Bauduin@cea.fr
- c. Sorbonne Universités, UPMC Univ Paris 06, CNRS UMR 8232, Institut Parisien de Chimie Moléculaire, 4 place Jussieu, F-75252 Paris Cedex 05, France

Experimental

Materials

Sodium chloride (NaCl, 99.5 %), Phosphotungstic acid hydrate (PW, MW = 3042 g/mol, $\text{H}_3\text{PW}_{12}\text{O}_{40} \cdot 9 \text{H}_2\text{O}$, 99.995 % purity), phosphomolybdic acid hydrate (PMo, $\text{H}_3\text{PW}_{12}\text{O}_{40} \cdot 9 \text{H}_2\text{O}$, MW = 1825 g/mol, 99.9 % purity) and silicomolybdic acid hydrate (SiW, $\text{H}_4\text{SiW}_{12}\text{O}_{40}$, MW = 3031 g/mol, $\text{H}_3\text{PW}_{12}\text{O}_{40} \cdot 14 \text{H}_2\text{O}$ 99.9 % purity) were purchased from Sigma Aldrich and were used without any further purification. $\text{K}_6\text{P}_2\text{W}_{18}\text{O}_{62} \cdot 14\text{H}_2\text{O}$ (KP2W, MW = 4597 g/mol)^[1] and $\text{K}_7\text{P}_2\text{W}_{17}\text{VO}_{62} \cdot 18\text{H}_2\text{O}$ (KP2WV, MW = 4503 g/mol)^[2] were prepared according to published procedures. The purity was checked by IR and ³¹P NMR spectroscopies and elemental analysis. The number of water molecules was determined for each polyoxometalate by thermogravimetry and was taken into account for the sample preparation. Milli-Q water was used with a permittivity lower than 10.5 $\mu\text{S}/\text{cm}$ and a total organic carbon content of 400 ppb.

Synthesis of $\text{H}_6\text{P}_2\text{W}_{18}\text{O}_{62} \cdot 31\text{H}_2\text{O}$ (HP2W, MW = 4369 g/mol) The acid form was prepared using the Drechsel method.^[3] A sample of the potassium salt (80 g) was dissolved in water (120 mL) under mild heating. After cooling, the solution was transferred to a separatory funnel, then ether (70 mL) and concentrated HCl (37%, 60 mL) were added. After shaking, the mixture separated into two phases on standing. The lowest phase was separated and transferred to another funnel and extraction was repeated by adding water (120 mL), ether (30 mL) and conc. HCl (40 mL). The lowest phase was separated, then extraction was completed by adding more HCl (40 mL) into the separatory funnel and the lowest phase was again collected. The latter evaporated by heating on a water bath, then the solution was left for crystallization on the bench top.

Anal. Found (%): W, 64.16; P, 1.28; H_2O , 11.31. Calcd for $\text{H}_6\text{P}_2\text{W}_{18}\text{O}_{62} \cdot 31\text{H}_2\text{O}$ (%): W, 67.16; P, 1.26; H_2O , 11.32.

NMR ³¹P (25 °C, 50% D_2O , referenced to external 85% H_3PO_4): -12.52 ppm.

FT-IR (KBr pellet, in cm^{-1}): 1090 (s), 962 (s), 914 (s), 780 (vs), 597 (vw), 564 (vw), 525 (w), 471 (vw), 359 (m), 324 (m)

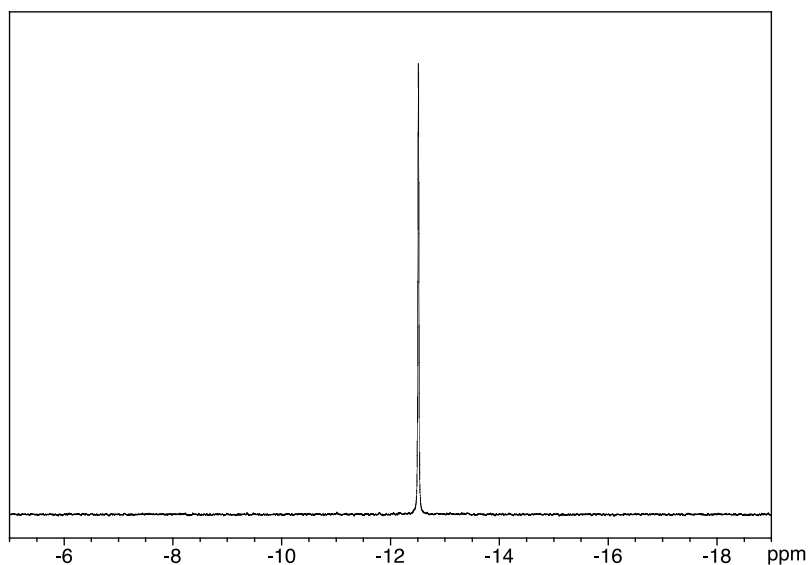


Figure S1: ³¹P NMR spectrum of $\text{H}_6\text{P}_2\text{W}_{18}\text{O}_{62}$ (HP2W) recorded in $\text{H}_2\text{O}/\text{D}_2\text{O}$ (50%)

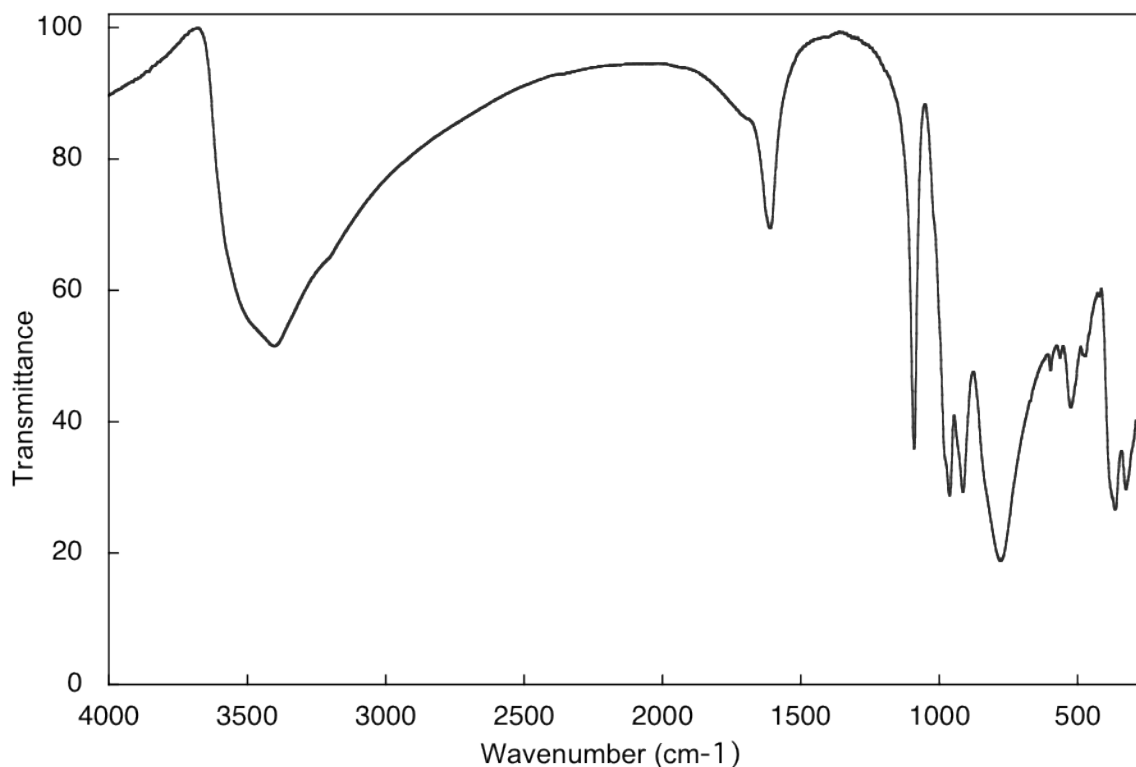


Figure S2: IR spectrum of $\text{H}_6\text{P}_2\text{W}_{18}\text{O}_{62}\cdot 31\text{H}_2\text{O}$ (HP2W) (KBr pellet)

- [1] Y. Sakai, S. Ohta, Y. Shintoyo, S. Yoshida, Y. Taguchi, Y. Matsuki, S. Matsunaga, K. Nomiya, *Inorg. Chem.*, **2011**, *50*, 6575-6583.
- [2] M. Abbessi, R. Contant, R. Thouvenot, G. Hervé, *Inorg. Chem.*, **1991**, *30*, 1695-1702.
- [3] E. Drechsel, *Ber. Chem. Ges.*, **1887**, *20*, 1452-1455.

CP measurements

Solutions containing 60 mM C_8EO_4 and a distinct amount of POM were placed into a thermostat (Thermomix_1460, B.Braun Melsungen AG) and were heated from 24 °C to 97 °C with a rate of 1 °Cmin⁻¹. The CP was detected by visual inspection with an uncertainty of $\pm 1^\circ\text{C}$.

SAXS

SAXS/WAXS experiments were performed at the TRUSAXS beamline (ID02) at the ESRF in Grenoble, France. The instrument uses a pin-hole collimated monochromatic incident beam with a wavelength $\lambda = 0.1$ nm (12.4keV). The SAXS detector (Rayonix MX-170HS) was set to a sample-to-detector distance of 1.2 m and WAXS data is simultaneously recorded with a Rayonix LX-170HS detector placed in air 14cm away from the sample. This setting allows to cover a broad q -range from 0.06 to 6.5 nm⁻¹ with $q = 4\pi/\lambda \sin(\theta)$, the scattering vector defined by the scattering angle 2θ . The magnitude of the q vector for the WAXS was calibrated with the Bragg-reflections of a Para Bromo Benzoic Acid (PBBA) standard. The flux of the incident X-ray beam was $6 \cdot 10^{12}$ photons/s. Samples were contained in quartz capillaries with a diameter of 2.0 mm and a wall thickness of 0.01 mm. Measured 2D scattering pattern were normalized to absolute scale (in mm⁻¹) after instrumental corrections and azimuthally averaged to obtain the scattered intensity as a function of q . The normalized cumulative background of water, sample cell and instrument were subtracted to obtain $I(q)$. Note that the beam polarisation was not taken into account during the data reduction.

Results

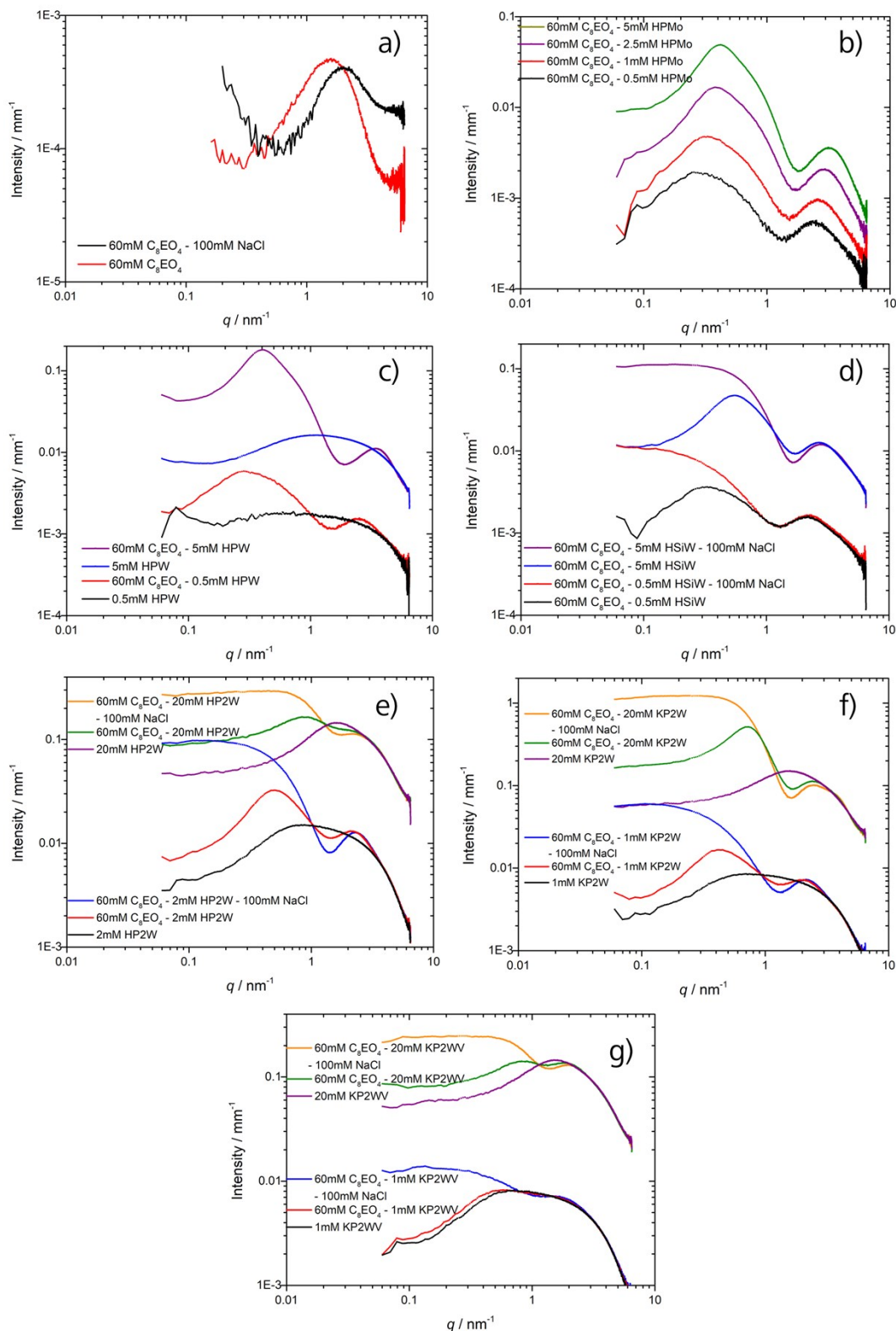


Figure S3: SAXS spectra of a) 60mM C_8EO_4 (with and without 100mM NaCl), b) aqueous solutions of 60mM C_8EO_4 with increasing concentration of $H_3PMo_{12}O_{40}$; c) aqueous solutions of 60mM C_8EO_4 with 0.5mM and 5mM $H_3PW_{12}O_{40}$; d) aqueous solutions of 60mM C_8EO_4 with 0.5mM and 5mM $H_4SiW_{12}O_{40}$ (with and without 100mM NaCl); e) aqueous solutions of 60mM C_8EO_4 with 2mM and 20mM $H_6P_2W_{18}O_{62}$ (with and without 100mM NaCl); f) aqueous solutions of 60mM C_8EO_4 with 1mM and 20mM $K_6P_2W_{18}O_{62}$ (with and without 100mM NaCl); g) aqueous solutions of 60mM C_8EO_4 with 2mM and 20mM $K_7P_2W_{17}VO_{62}$ (with and without 100mM NaCl).

Small angle X-ray measurements (SAXS) were performed on C₈EO₄, POMs and their mixtures to investigate the adsorption of POMs on the micellar surface, see Fig. S3. The scattering pattern of 60mM C₈EO₄ is of very low scattered intensity, below 10⁻³ mm⁻¹, as expected from the very low contrast of micelles against water and their small size.¹ The large oscillation centred at around 1.5 nm⁻¹ is related to the micelle form factor. This feature in the spectrum originates mainly from an excess in the electron density in the micellar shell, due to the presence of EO groups that have an electron density higher than the micellar core (octyl chains) and the surrounding medium (water). The very low scattering intensity for $q < 1.5 \text{ nm}^{-1}$ indicates that the overall electron density of the micelle (core + shell) is comparable to the one of water, i.e. the micelle/water contrast is very weak. All Dawson and Keggin POMs display the scattering signature of dispersed spheroidal objects in aqueous solution with electrostatic repulsions, indicated by the decrease of the scattered intensity for $q < 0.5 \text{ nm}^{-1}$. The SAXS spectrum for the mixture of 60mM C₈EO₄ and POMs display a much higher scattered intensity and a completely different pattern indicating a core-shell structure with a large electron density excess in the shell, i.e. C₈EO₄ micelles with POMs adsorbed in the micellar shell. Strong inter-micelle and inter-POM repulsions account for the depression of the scattered intensity for $q < 0.4 \text{ nm}^{-1}$. The addition of 100 mM NaCl to solutions containing 60mM C₈EO₄ and POMs, aiming at screening electrostatic interactions, leads to an increase of the scattering intensity for $q < 0.4 \text{ nm}^{-1}$. Such a SAXS pattern informs therefore on the strong adsorption of POMs onto the surface of C₈EO₄ micelles as shown previously by Naskar et. al for HSiW-C₈EO₄ in comparable compositions.¹ A similar fitting procedure was applied on the SAXS spectra obtained with Dawson POMs in the presence of 100 mM, see the details in the following section.

SAXS modelling

SAXS spectra of C₈EO₄ micelles in the presence of Dawson POMs and 100mM NaCl, were modelled by a fitting procedure previously described for C₈EO₄-SiW₁₂O₄₀ micelles in Naskar et al.¹ In this fitting procedure the scattered intensity was considered as a sum of contributions from micelles, POMs and background as:

$$I(q) = I_{POM} + I_{micelles} + Bkg \quad \text{Eq. (1)}$$

The contributions of the POMs and micelles were expressed as:

$$I(q) = n_{POM} V_{POM}^2 (SLD_{POM} - SLD_{water})^2 P_{sphere}(R_{POM}, q) S_{HS}(q, \varphi^{POM}, R_{HS}^{POM}) + n_{micelles} P_{core-shell-ellipsoid}(a, b, c, dR, SLD_{core}, SLD_{shell}, q) S_{HS}(q, \varphi, R_{HS}) + Bkg \quad \text{Eq. (2)}$$

with n , the particle concentrations, V , the volume of the particles, SLD , the scattering length density which is related to the electron density, P and S , the form and structure factors that take into account the shape of the particles and the inter-particles interactions. A spherical form factor, P_{sphere} , and a triaxial-ellipsoid core-shell form factor, $P_{core-shell-ellipsoid}$, were used to describe the shapes of (i) the POMs with a radius, R_{POM} , and (ii) the micelles with a radius of the core, R , and a shell thickness, dR . Interactions between POMs were taken into account with a hard-sphere structure factor, $S_{HS}(q, \varphi^{POM}, R_{HS}^{POM})$ and $S_{HS}(q, \varphi, R_{HS})$ respectively between POMs and between micelles, with R_{HS} , the hard-sphere radius, and φ , the volume fractions.

The scattering length density (SLD) used in the model are: $SLD_{water} = 9.398 \cdot 10^{10} \text{ cm}^{-2}$ water being considered as the surrounding medium and the SLD of the core, $SLD_{core} = 9.129 \cdot 10^{10} \text{ cm}^{-2}$, that was taken to be SLD value of C₈EO₄. SLD_{water} and SLD_{core} are fixed and therefore used as input parameters. For comparison, the SLD values of POMs are around six to ten times higher than $SLD_{water/C8E4}$, for example $SLD_{PW12O40} = 86.9 \cdot 10^{10} \text{ cm}^{-2}$, as expected from the high POM density and from the presence of W which has a high electron number ($Z_W = 74$). Consequently, the scattered intensity of C8E4-POM mixtures in the low q -regime mainly arise from the POMs that decorate C₈EO₄ micelles. In the presence of 100mM NaCl, i.e. with most of the electrostatic repulsions being screened, the scattered intensity in

the low q -range for POM-decorated micelles is then around ten times the one of the POMs in water. The most influent parameters on the shape of the scattering spectra SLD_{shell} , a , b , c , dR , R_{POM} and the pre-factors, n , are fitted with constraints on the micellar size, i.e. (1) dR is around the size of the POM, here from 1 to 1.7 nm for Dawson POMs, (2) a , b , c values are above the length of a C_8 alkyl chain (1.1 nm), (3) at least a , b , or c must range between the length of a C_8 alkyl chain (1.1 nm) and the C_8EO_4 length (2.6 nm) as the 3D swelling (a , b , and $c > 2.6$ nm) of the micelle has no physical meaning. Compared to the previous investigation by Naskar et al., the micelles are fitted here with a triaxial ellipsoid model, and not a simple spherical model, as it enables a better fitting of the data. The ellipsoid model accounts for small anisotropy in the micelle shape and may also describe small polydispersity in the micellar size.

The SAXS spectra could be well fitted in absolute scale using this procedure, see Fig. S4. The pertinent fitting parameters are listed in Table S1. As previously observed C_8EO_4 - $SiW_{12}O_{40}$ micelles, SLD_{shell} is found to be much higher than SLD_{core} and SLD_{water} indicating a strong electron density excess in the shell that can only be explained by the presence of POMs in the shell. Indeed, the POMs are the only components in the systems that have a high electron density able to produce such large electron density excess in the shell. It is therefore concluded from the micellar size parameter (a , b , and c) and from SLD_{shell}/dR values that POMs are located around C_8EO_4 micelles with partial or total penetrations of the POMs in the EO chains, as a , b , c values around the length of C_8 alkyl chain.

Table S1: Results of the fitting of SAXS of Dawson POMs-C8E4 systems with 100 mM NaCl solution at 23 °C, with a , b , c the radii of the micellar core using a triaxial ellipsoid geometrical model, dR the shell thickness (composed of POMs, water and EO moieties), SLDs the scattering length densities, $S(q)_{POM}$ and $S(q)_{micelle}$ the structure factors taking into account for POM-POM interaction and micelle-micelle interactions.

	Form and structure factors parameters									
	a	b	c	dR	SLD_{core}	SLD_{shell}	$S(q)_{POM}$		$S(q)_{micelle}$	
	nm	nm	nm	nm	$\text{cm}^{-2} \cdot 10^{-10}$	$\text{cm}^{-2} \cdot 10^{-10}$	Φ	R_{HS}	Φ	R_{HS}
⁽¹⁾ 60 mM C ₈ EO ₄ + 10mM H ₄ SiW ₁₂ O ₄₀	1.61	1.61	1.61	0.80	9.1	16.9	0.152	0.84	0.035	3.90
60 mM C ₈ EO ₄ + 2mM H ₆ P ₂ W ₁₈ O ₆₂	1.13	1.13	1.46	1.7	9.1	16.7	0.155	1.1	0.0105	1.8
60 mM C ₈ EO ₄ + 20 mM K ₆ P ₂ W ₁₈ O ₆₂	1.1	1.1	0.9	1.5	9.1	14.5	0.165	0.76	0.031	6.0
60 mM C ₈ EO ₄ + 20 mM K ₇ P ₂ W ₁₇ VO ₆₂	1.25	1.25	1.25	1.7	0.91	16.0	0.09	1.0	0.165	2.3

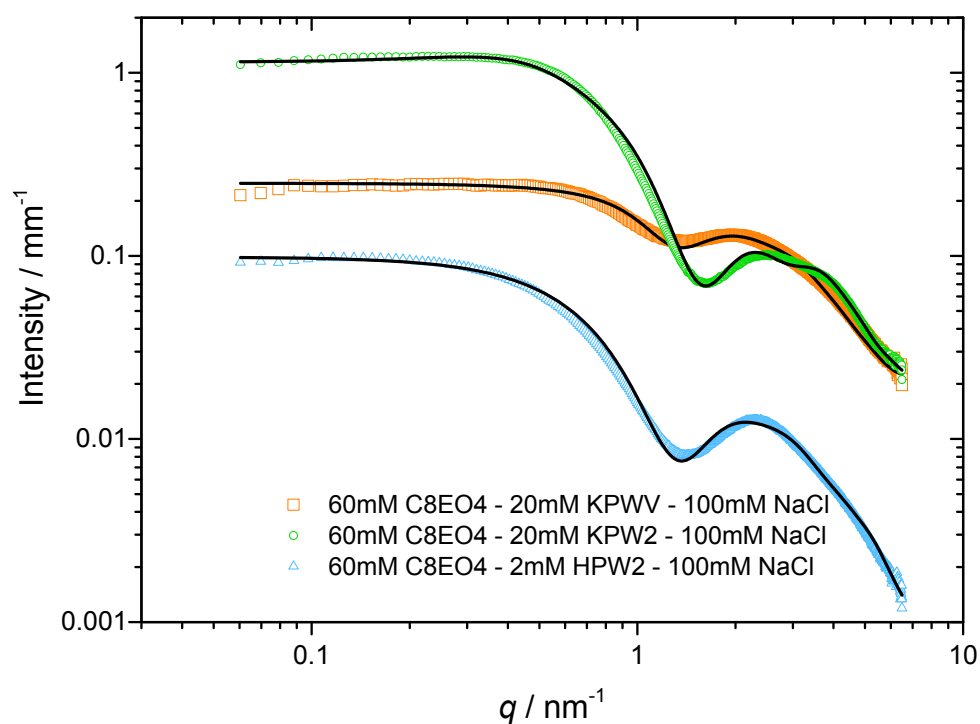


Fig. S4 SAXS spectra of C_8EO_4 60mM in the presence of Dawson's POMs and 100 mM NaCl. Full lines are the best fit obtained from the POM decorated micelle model, i.e. core-shell triaxial ellipsoid model with electron density excess in the shell, described in the text.

1 B. Naskar, O. Diat, V. Nardello-Rataj and P. Bauduin, *J. Phys. Chem. C*, 2015, **119**, 20985–20992.

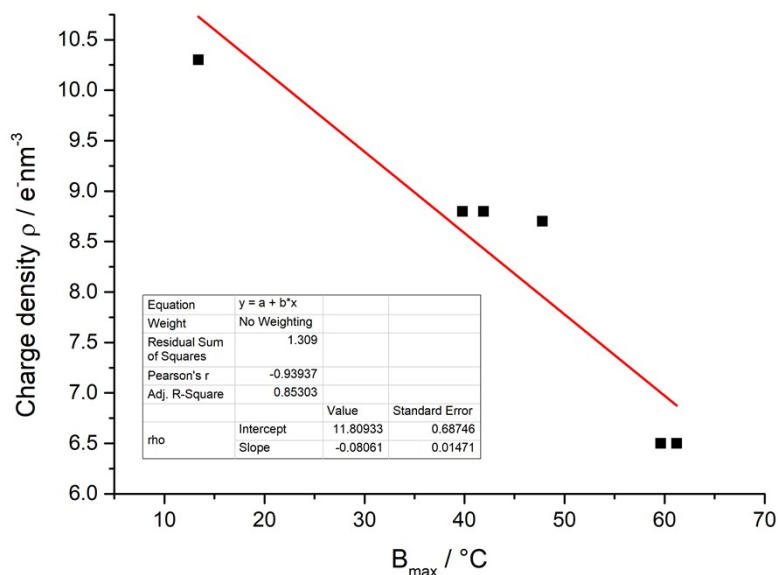


Figure S5: ρ vs B_{\max} shows roughly a linear evolution, with a coefficient of determination for a linear fit of $R^2 = 0.85$ (see Fig. S2).

This linear relationship between B_{\max} and the charge density suggests that the charge density is a major feature of POMs that controls their chaotropic behaviour.